SHALLOW GEOLOGICAL STRUCTURES OF THE SOUTH SHETLAND TRENCH, ANTARCTIC PENINSULA

Filomena M. Loreto*,[✉]**, Bruno Della Vedova****, **Flavio Accaino***, **Umberta Tinivella*** and **Daniela Accettella***

* *Istituto Nazionale di Oceanografia e Geofisica Sperimentale (OGS), Trieste, Italy.*
** *Dipartimento di Ingegneria Civile e Ambientale (DICA), Università di Trieste, Italy.*
✉ *Corresponding author, e-mail: mfloreto@ogs.trieste.it.*

Keywords: *morpho-structures, oblique fault systems, transform faults, differential sinking, passive subduction, Phoenix Plate.*

ABSTRACT

In order to study the differential passive subduction among the three oceanic segments of the Phoenix Plate remnant, the R/V OGS-Explora acquired new geophysical data in the South Shetland Trench (offshore to the Antarctic Peninsula).

An integrated geophysical dataset was acquired in the trench across the incoming oceanic plate segmented by the "D" and "E" oceanic Fracture Zones, and along the frontal part of the Antarctic Peninsula accretionary prism. We present here a high resolution multibeam bathymetry map, Chirp sub-bottom profiles and marine magnetic data to study changes in the deformational style along strike and to better understand features and processes of passive subduction.

The new multibeam image and Chirp data display in detail shallow structures affecting the seafloor as a response to crustal deformation. Normal faults, bounding horst and graben structures cutting the incoming plate, are detected and characterized by variable orientation with respect to the inferred "D" and "E" Fracture Zones. Normal faults, width and depth of the trench and morphology of the frontal prism are related to bending and roll-back of the Phoenix Plate, and to inherited structural discontinuities. Some of these oblique faults offset the seafloor, with variable throws and with local dip changes.

The orientation of the oblique faults, the different depth of the three oceanic segments and narrowing and deepening of the trench indicate that differential coupling between the Hero, Shackleton, "E" and "D" Fracture Zones may locally modify the regional stress field orientation and the sinking of each oceanic segment, during bending and roll-back.

INTRODUCTION AND TECTONIC SETTING

The passive subduction of oceanic lithosphere is an interesting case of study, because the pull-down forces of the dense subducting slab still continue to act when active spreading, at the mid ocean ridge, ceases. This change in the stress regime at convergent margins induces a significant tectonic relaxation in the subducting plate and back-arc areas.

Passive subduction implies bending and roll-back of the oceanic lithosphere (Royden, 1993). Generally, the extension rate affecting back-arc basins balances the seaward moving rate of the trench axis, as observed along the Carpathian-Pannonian system (Royden, 1988; Nemcok et al., 1998) and the Thailand Basin (Morley, 2001). The extension affecting the oceanic plate is mainly represented by normal faults, associated to horst and graben structures (Masson, 1991). These structures are observed along the northern Chilean margin (Scholl et al., 1970; Schweller and Kulm, 1978; Carbotte and Macdonald, 1994) and along the Japan trench (Kobayashi et al., 1998), with variable orientation respect to the margin strike (Kobayashi et al., 1998; von Huene and Ranero, 2003; Ranero et al., 2003). Moreover, the presence of morphologic roughness on the incoming oceanic plate (horsts, grabens and seamounts) can significantly alter the geometry and morphology of the trench and at the frontal part of the accretionary prism, inducing local deformation and tectonic erosion (Hilde, 1983; von Huene, 1986; Ballance et al., 1989). In this context, the mechanical response of the oceanic plate, segmented by transform faults, could laterally change because of the different age and physical properties pertaining to each subducting lithospheric segment.

The passive subduction analysis, of the last Phoenix (PHO) Plate segment beneath the South Shetland continental margin, offers the opportunity to study the shallow deformation in the trench. The PHO Plate is the last remnant of the Nazca Plate subduction beneath of the Antarctic (ANT) Plate, bordered by the Hero, to the SW, and by the Shackleton Fracture Zones (FZs) to the NE (Fig. 1; Sandwell and Smith, 1997). The structural complexity of the Pacific margin of the Antarctic Peninsula (AP) is caused by the long lived tectonic history of the ridge-trench collisions progressing from the SW to the NE (Barker, 1982; Larter and Barker, 1991). Nazca Plate subduction was active along the Pacific margin of Gondwana Land from the late Paleozoic time (Pankhurst, 1990) to 4 Ma (Larter and Barker, 1991), when spreading at the ANT-PHO Ridge ceased (GRAPE Team, 1990). This hypothesis is confirmed by the absence of significant seismicity along the ANT-PHO Ridge (box in Fig. 1); instead recent seismic events recorded within the fore-arc region of the South Shetland (see box included in Fig. 1; and website http://epsc.wustl.edu/seismology/SEPA) indicate that the subduction zone is still active (Robertson Maurice et al., 2003). The Shackleton FZ along the northeastern side is active (Thomas et al., 2003), whereas the Hero FZ along the southwest side is locked (Barker, 1982). The surface projection of these two main fracture zones are also delimiting the lateral extent of the Bransfield Microplate (Lawver et al., 1995), which is separated from the AP by the opening of the back-arc basin and related to the ridge spreading cessation (Barker and Dalziel, 1983). The Bransfield Microplate is moving seaward with a convergence rate of about 1 cm/yr or slower (Dietrich et al., 2001; Smalley et al., 2003).

The passive subduction at the South Shetland trench is characterized by: 1) geometry of subduction with an angle of incidence that progressively decreases moving from the Hero towards the Shackleton FZ; 2) bending and roll-back of the oceanic plate due to the cessation of ANT-PHO spreading centre; 3) extensional regime in the incoming oceanic plate (caused by the stress relaxation); 4) opening of the Bransfield Strait back-arc basin.

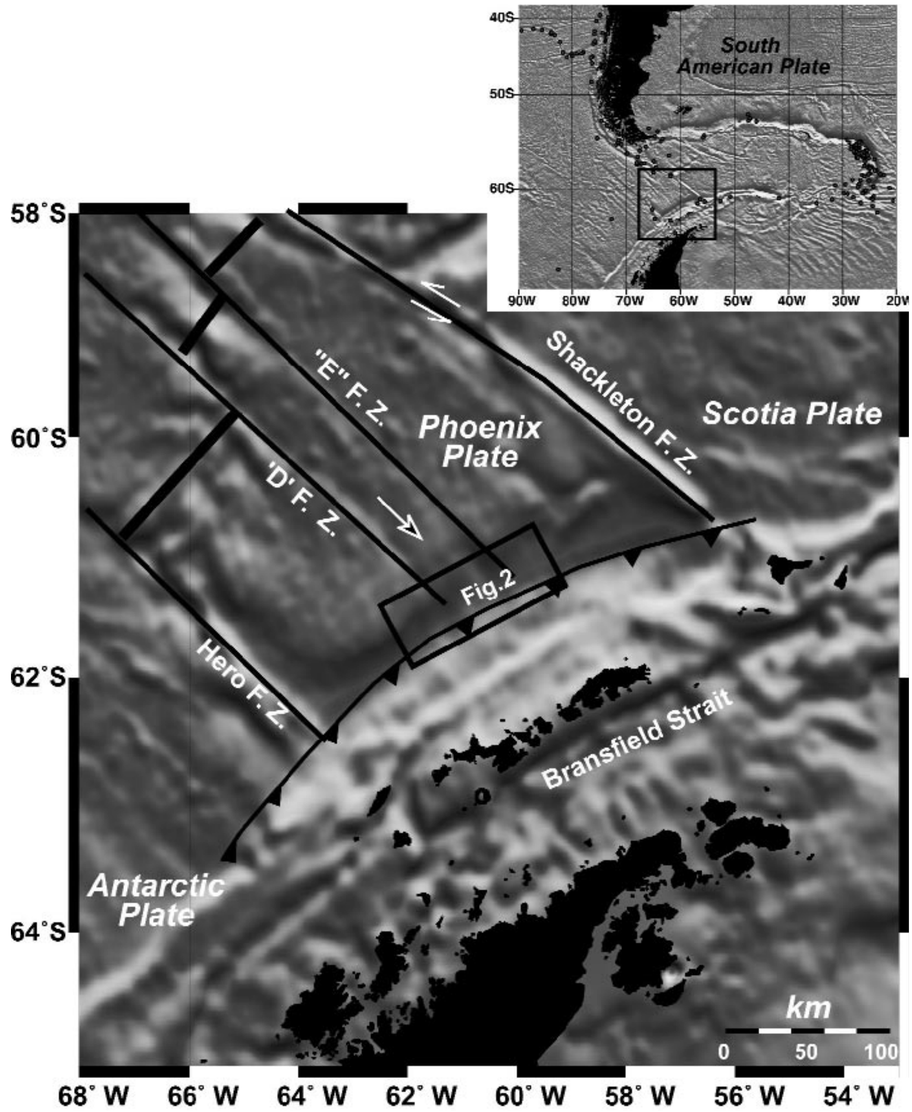

Fig. 1 - Shaded relief morpho-structural map of the subducting Phoenix Plate (modified from Sandwell and Smith, 1997). The solid rectangle indicates the study area; the single arrow indicates the direction of plate convergence; coupled arrows indicate the left-lateral transcurrent movement along the Shackleton Fracure Zone (FZ). The inset box shows the seismicity with black dots (derived by the web site http://www.seismology.harvard.edu/CMTsearch.html).

The PHO oceanic plate remnant is segmented into 3 main blocks (Barker, 1982) by the “D” and “E” FZs (Fig. 1). The age of the oceanic lithosphere entering the subduction zone increases from 14 Ma (to the SW) to about 23 Ma (in the NE), according to magnetic chrons identification (Larter and Barker, 1991). This is also confirmed by the distance between ANT-PHO Ridge segments and the South Shetland Trench, and the obliquity of the subduction with respect to the margin. Each segment is characterized by different properties, such as: thickness, density, elastic thickness and rigidity. These differences are recorded by (i) lateral variability of the trench and prism morphology, (ii) plate tectonic setting (Kim et al., 1995), (iii) sediment blanketing, (iv) deformation of the continental margin and (v) associated magmatism (Hawkes, 1981). In particular, different strain patterns should be expected to affect the subducting oceanic segments, if each of them is controlled by its elastic properties. In order to test these hypotheses in the study area (Fig. 1), an integrated geophysical cruise was performed during the Antarctic summer 2003-2004, onboard R/V OGS Explora. Data were collected as part of the Program SLAPPSS (Subduction of the LAst Phoenix Plate segments beneath the South Shetland margin, Antarctic Peninsula), supported by the Italian Programma Nazionale di Ricerche in Antartide (PNRA). The geophysical dataset is composed by high-resolution multibeam bathymetry, Chirp profiles, magnetic measurements, reflection and refraction (Ocean Bottom Seismometer) seismic data. In this paper we present multibeam bathymetry, Chirp profiles and a magnetic profile to analyse the shallow geological structures.

GEOPHYSICAL DATA ACQUISITION AND PROCESSING

Multibeam bathymetry data

The high-resolution bathymetry was acquired using the new Seabat 8150 multibeam system on the OGS Explora, with a nominal depth range of 0.1-15 km, 234 beams and a nominal frequency of 12 kHz. Data acquisition and processing was performed using the PDS2000 software, that allowed us to produce a high resolution bathymetric image of about 9.700 km^2 (Fig. 2). The acquisition was completed with 7 swaths parallel to the trench axis. The swath coverage is about 10 km across considering about 15% for swath overlap, which corresponds to 2.5 times the water depth. The maximum depth exceeds 5000 m. The sea water velocity was measured by 4 CTD probes in the water column. Editing of the navigation and filtering on raw data were applied to remove noise. The horizontal resolution, which corresponds to the grid cell size, is about 150 m, whereas the vertical resolution is about 20 m.

Sub-bottom Chirp data

About 1000 km of Chirp profiles were acquired, along the multibeam passages. The CAP-6600 Chirp II, with 16 transducers and 2-7 kHz of sweep, was used. The sonar operating frequency is 7 kHz and the maximum nominal penetration is about 100 m in soft sediments.

The Chirp provides instantaneous amplitude records, that allow image processing of the data. The output traces had to be set to constant sampling number, with starting time acquisition equal to zero and variable end time, according to the water depth. Thus, the resolution of acquired data is a function of the total depth; the sampling rate is 0.533 ms and the uncertainty is in the order of one meter. A sea bottom mute and a weighted moving average on a panel consisting of seven traces were applied to the data to improve the lateral coherence and the signal to noise ratio. The low quality of data is due to the loss of high frequencies and to the impossibility to select an appropriate sampling rate. All Chirp images, shown in the figures, were processed using the Seismic Unix (Cohen and Stockwell, 2003) free software package and plotted using the same vertical exaggeration.

Magnetic profiles

Magnetic profiles were collected during the bathymetric survey by using the Sea Spy Magnetometer, which is characterized by an operating range of 18000-120000 nT, a resolution of 1 nT and a sample frequency of 4-0.1 Hz. Data processing is not shown here, because the target of this study to analyse the main shallow structural trend of the South Shetland trench area.

RESULTS

The integrated analysis of multibeam bathymetry, sub-bottom and the magnetic profile lead us to: 1) image the main investigated areas (the incoming oceanic plate, the trench and the outer accretionary prism); 2) highlight the morpho-structural elements that record the passive subduction of the last PHO Plate segments; 3) understand the tectonic relationship between investigated zones and shallow deformations associated to the passive subduction mechanism.

Morphology of the investigated area

The high resolution bathymetric map (Fig. 2) reveals the morphology of the three main areas in the South Shetland trench:

– the <u>outer rise of the oceanic plate,</u> characterized by basaltic rocks of MORB affinity, is covered with a limited thickness of pelagic and hemi-pelagic sediments;

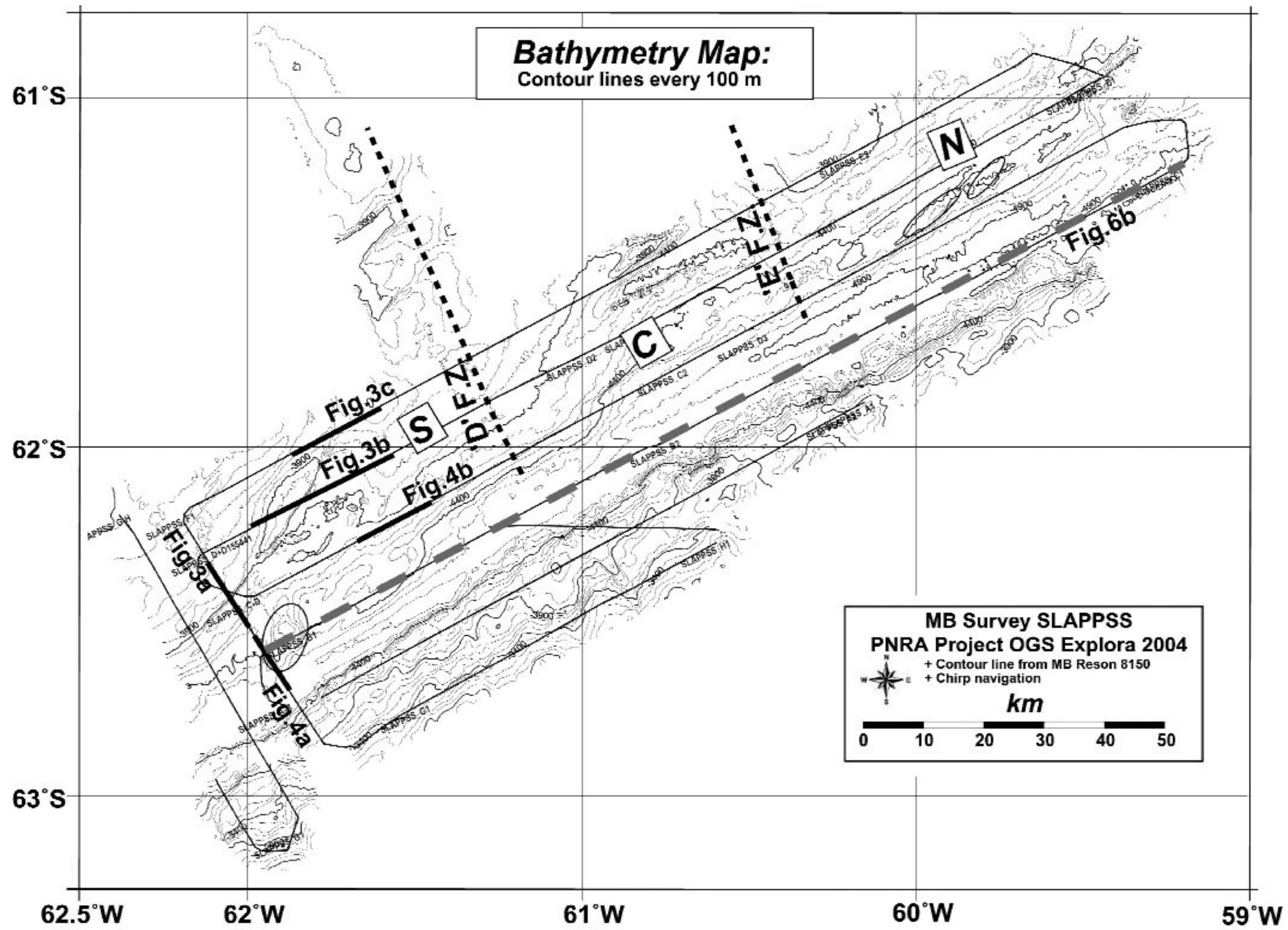

Fig. 2 - High resolution bathymetric map (Multibeam image) of the investigated area. S- Southern; C- Central; and N- Northern segments. Thin lines indicate all Chirp profiles; thick black lines indicate the location of Chirp profiles analysed in this paper and displayed in Figs. 3 and 4. Dashed grey line indicates the location of the magnetic profile displayed in Fig. 6b. Ellipses border morphological highs.

– the South Shetland trench axis is characterized by an irregular shape and geometry (Fig. 2), and is filled by turbiditic and hemi-pelagic sediments;
– the frontal part of the upper plate, which corresponds to the frontal accretionary prism, is characterized by a fairly linear continent-ocean boundary and by accumulation of off-scraped trench sediments.

Outer rise of the oceanic plate

The average depth of the oceanic domain, on the outer trench side, decreases from the trench towards the outer rise of the oceanic plate (Fig. 2) and, generally, is larger in the central segment than in the adjacent segments. The investigated area includes the “E” and “D” FZs (Fig. 1), that divide the oceanic plate in three main segments here indicated as Southern, Central and Northern segments (Fig. 2). The “E” and “D” FZs do not have clear expression on the high-resolution bathymetry map, consequently their location and orientation were derived from the bathymetry estimated from altimetry and from gravimetry anomalies (Fig. 1).

Several morphologic features, represented by highs, elongated ridges and troughs, characterize the Southern segment. A seamount, located on the oceanic plate next to the trench Fig. 2), is interpreted as a volcano, due to its conic shape and to a small depression on its top (interpreted as a crater). The volcano was named “Explora” and is approximately 0.5 km high and 7 km wide. The seafloor morphology of the Central oceanic segment is smoother and locally deeper than surrounding areas, and is interrupted by a narrow and elongated morphologic high, oriented quasi-orthogonal to the ”D” and “E” FZs. The Northern segment morphology is characterized by many elongated highs, slightly oblique with respect to the continental margin. The shape of some of these highs suggests that their origin is likely volcanic (Fig. 2).

On the whole, the oceanic domain is affected by a widespread pattern of oblique lineaments, cutting across all three segments with variable orientation. In the Southern segment the lineaments show a NE trend, making an angle of about 53° with respect to the direction of the “D” FZ (Fig. 2). The “Explora” volcano is located on one of these lineaments and shows a clear normal fault, splitting the edifice and the top caldera in two. In the Central segment these lineaments decrease in number to one or two, and are generally characterized by a smaller relief and display an orientation almost orthogonal to the FZs. In contrast, in the Northern oceanic segment they become more abundant, closer spaced and obliquely oriented, with an angle of about 72° respect to the “E” FZ.

South Shetland trench

The trench is irregular in shape and depth: it is wider and reaches about 5000 m of maximum depth (Fig. 2) in its northeast part, whereas, in the southernmost part, close to the “Explora” volcano location, it is very narrow and about 4700 m deep. Therefore, the trench deepens slightly north-east-ward. Narrow morphological irregularities, likely due to erosion of bottom currents, characterize the trench and are smoothed by sedimentary infill. On the ocean side, the trench is characterized by an irregular shape and zigzag trend geometry (Fig. 2). In the Southern segment the axial trench is very narrow and the frontal part of the accretionary prism shows a landward indentation, of about 3 km, with respect to the regional trend.

Frontal part of the upper plate (accretionary prism)

The outer front of the accretionary prism is a linear regional feature that represents the plate boundary between the PHO Plate and the Bransfield Microplate. It is generally characterized by short wavelength morphological lobes, separated by narrow and deep canyons descending along the slope orthogonal to the trench axis (Fig. 2). The multibeam survey area was not large enough to image the entire accretionary prism, but, on the base of previously published seismic data (Kim et al., 1995; Aldaya and Maldonado, 1996) it should be relatively narrow (in the range of 10-20 km).

Sub-vertical fault scarps and throws

In spite of the low penetration and limited spatial resolution of sub-bottom profiles, sub-vertical scarps and throws along the main morpho-structural lineaments were clearly detected and shown on the multibeam bathymetry map. The most relevant lineament within the entire investigated area is located in the Southern segment. From southwest to northeast, it shows significant vertical displacement of the seafloor, with the down wall side generally facing the trench (towards SE). The largest throw was observed along the Chirp line F1 (Fig. 2), with a vertical displacement of about 0.22 s (one way travel time) near shot point (s.p.) 420 (Fig. 3a), showing a deep of about 320 m (assuming a seawater sound velocity of 1470 m/s). In this case, the scarp repre-

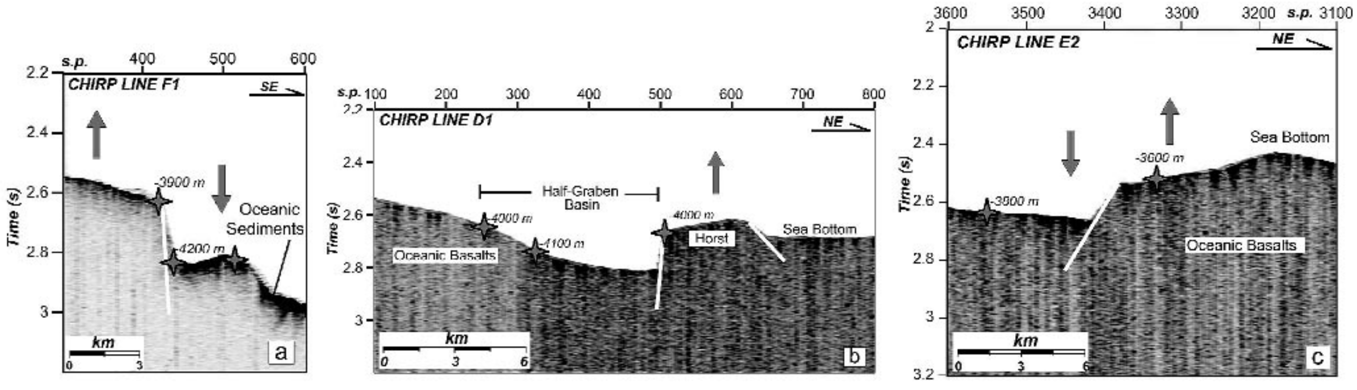

Fig. 3 - a: Chirp line F1. Thick arrows indicate relative movements of faulted oceanic sediments. The fault plane is indicated with the white line; the maximum offset of the seafloor is about 320 m. b: Chirp line D1 located northwards (Fig. 2); the maximum offset of seafloor is about 220 m in correspondence of s.p. 500. c: Chirp profile E2, the maximum offset is about 180 m.

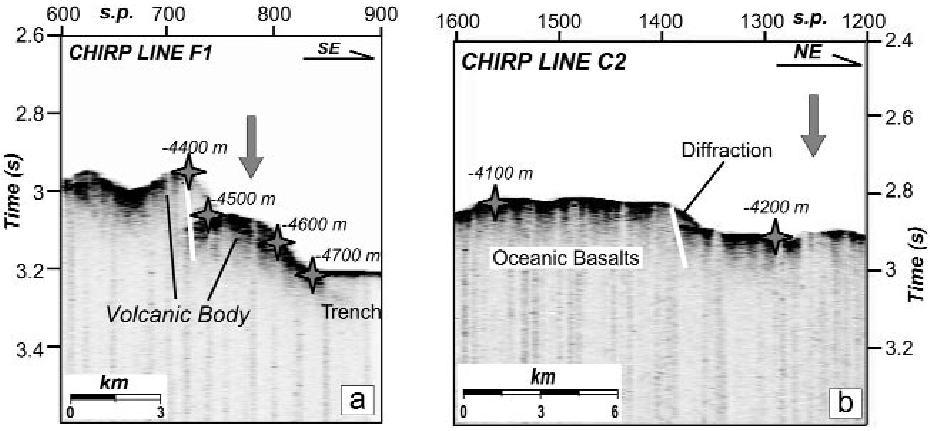

Fig. 4 - a: Chirp profile F1 located close to the trench; thick arrows indicate the relative movement along a normal fault indicated with a white line; the maximum offset of the seafloor is about 160 m. b: Chirp profile C2; the white line indicates the probable fault or morphological discontinuity showing maximum offset of about 60 m.

sents a sub-vertical normal fault southeast-ward dipping. This extensional fault is quite continuous and can be followed farther to the N (Fig. 2). On the Chirp line D1, near s.p. 630 (Fig. 3b), the down wall throw dipping to the SE is reduced to about 40 m, whereas near s.p. 500 the down wall throw slightly dipping northwest-ward shows an offset of about 220 m. A basin (half-graben type), about 7.5 km wide between s.p. 250 and 500 (Fig. 3b), is bordered on one master side by this fault which controls its opening. This is deduced by the -4000 m bathymetry contour line trend (Fig. 2) and by the scarp fault detected on the Chirp lines (Figs. 3b and 3c).

Moving to the north, along the Chirp profile E2 (Fig. 3c), the down wall is still dipping to the NW, but with a reduced offset to about 170 m. Probably this major fault continues northwards with a decreased offset and stops in correspondence of the "D" FZ, as suggested by the shape of -4000 m contour line (Fig. 2).

In the Central segment no evident bathymetric lineaments are recorded and only one small ridge is present, oriented parallel to the trench axis as suggested by the depth contour lines (Fig. 2). In the Northern segment the bathymetry is characterized by a linear trend oriented slightly oblique to the trench axis (Fig. 2).

The newly discovered "Explora" Volcano (Fig. 2) is cut by a normal fault, detected on the Chirp line F1 (Fig. 4a), which offsets the seafloor of more than 100 m toward the trench. By integrating the multibeam image with the sub-bottom profile it is possible to reconstruct the shape of the edifice and to map the direction of the normal fault. This fault that cut the volcano was recorded on s.p. 720 and partially obscured by diffractions. This normal fault offsets the irregular seafloor morphology by more than 150 m, slightly dipping to the southeast-wards. The acoustic reflectivity of the volcano is higher than that of the trench sediments to the SE, suggesting petrophysical differences between the two areas. The seafloor offset related to the normal fault abruptly decreases to a few meters towards NE, as shown by Chirp line C2 (Fig. 4b).

DISCUSSION

The bathymetric survey and Chirp profiles show the presence of new extensional elements, such as the oblique lineaments and the spatially associated young volcanic edifices on the oceanic domain. These features represent the surface expression of the plate bending and roll back of the PHO oceanic Plate. The subduction is tightly constrained by the boundary conditions represented by the Shackleton and Hero FZs. The bounding FZs, together with the recent subduction history of the PHO Plate, have an important role on the fate and evolution of the oceanic plate remnant. The combination of subduction rate, geometry (direction of convergence, different age of segments) at the South Shetland Trench, and stress regime across the adjacent boundaries likely control the bending of the oceanic plate, as well as the shape of the trench and of the accretionary prism along the AP margin. These new elements and observations improve previous structural analysis (Kim et al. 1995; Aldaya and Maldonado, 1996; Larter and Barker, 1991) and allow us to propose a new geological model.

Shallow morpho-structures of the subducting plate

The Multibeam bathymetry reveals the morphology of a limited portion of the South Shetland Trench, showing in detail its extension and character.

The bathymetry of the oceanic domain across the three segments, at about the same distance from the trench, shows a regional pattern characterized by a greatest depth in the central oceanic segment. The seafloor depth slightly decreases in both directions moving away from the central segment. This observation is confirmed by previous studies (Lodolo et al., 2002; Kim et al., 1995) and could be extrapolated, with local differences, to the top of the oceanic crust entering the subduction zone. The Southern and Northern segments show normal faults, forming an angle with the trench and plate bending axis, and are characterized by a shallower and rougher seafloor morphology with respect to the Central segment, where a single ridge parallel to the trench axis was detected. These morphological and structural elements suggest that the stress field affecting the bending of the oceanic plate changes from one segment to the other across the "D" and "E" FZs, which are likely characterized by a weak coupling.

The trench is still evolving after the stop of the ANT-PHO Ridge active spreading and is filled by Middle Miocene to present sediments (Camerlenghi et al., 1997; Rebesco et al., 2002). Despite the stop of spreading, the deformation of the recent sedimentary sequences, imaged by seismic sections across the South Shetland Trench (Lodolo et al., 2002; Kim et al., 1995), and by the seismicity recorded in the area (Pelayo and Wiens, 1989; Larter, 2001; see the website http://epsc.wustl.edu/seismology/SEPA), confirms that the subduction is continuing, as a probable consequence of the slab pull-dawn sinking and of the push of the Bransfield Microplate towards NW (Dietrich et al., 2001; Smalley et al., 2003).

The morphology of the trench ocean side is locally controlled by the recent oblique fault pattern, as suggested by its sharp bends in correspondence of these lineaments (Fig. 5). Moreover, the trench morphology could be partially controlled by the presence of "D" and "E" FZs, that favour the differential sinking of each oceanic segment and by the northward regional trench widening, even if the FZs are not located in correspondence of the main sharp bends (Figs. 2 and 5). The oceanic crust, to the south, is younger and consequently the sinking would be smaller; in fact, the Hero FZ is a discontinuity that separates the southern locked to the northern passive subducting margin, whereas the Shackleton FZ separates two plates that are still moving (Thomas et al., 2003) allowing the sinking of the Northern segment. The local narrowing of the trench, in the southern segment, could also be partially due to the "Explora" Volcano (Fig. 5), which is approaching the trench axis. The seamount, interacting with the frontal prism before being subducted, can produce the narrowing of the trench, as observed along many circum-pacific margins (Fisher et al., 1998; Ranero and von Huene, 2000; Lallemand et al., 1994) and by laboratories experiments (Dominguez et al., 2000).

In the Southern segment the trench is narrower and shallower than in the Northern segment due to the (i) different buoyancy, (ii) relative movements along the lateral plate boundaries (Hero and Shackleton FZs) and (iii) oceanic roughness. In the Northern segment, the trend and character of the outer deformation front is represented by elongated ridges and small lobes affecting trench sediments trough thrust faults (Fig. 5). The young ridges are likely the bathymetric expression of trench sediments scraped off and piled up onto the top of the main decollement, as observed in other accretionary prisms: Southern Chile (Loreto, 2005), Southern Barbados (Huyghe et al., 2004) and Nankai (Gulick et al., 2004). An other possible explanation about the morphology of the frontal prism could be that it is produced by slumping of unstable sediments and by a meandering of the bottom current stream.

The morphology of the frontal prism is incised by narrow and deep canyons, crosscutting orthogonally the accretionary wedge (Fig. 5). They probably cut the entire continental slope, from the shelf break down to the trench, and are incised by erosional turbiditic currents characterized by high density and velocity. These currents can be associated to mass wasting of glacial sediments during the Upper Quaternary glacial and interglacial periods, as analysed along peri-Antarctic margins (Pudsey and Camerlenghi, 1998; Kuvaas et al., 2005). The location of the deep canyons could be also controlled by tectonic lineaments, such as those in correspondence of the subducted transform faults (Fig. 2).

Oblique lineaments affecting the segmented oceanic crust

The joint analysis of the bathymetric map and Chirp data reveals the presence of a newly recognised structural pattern

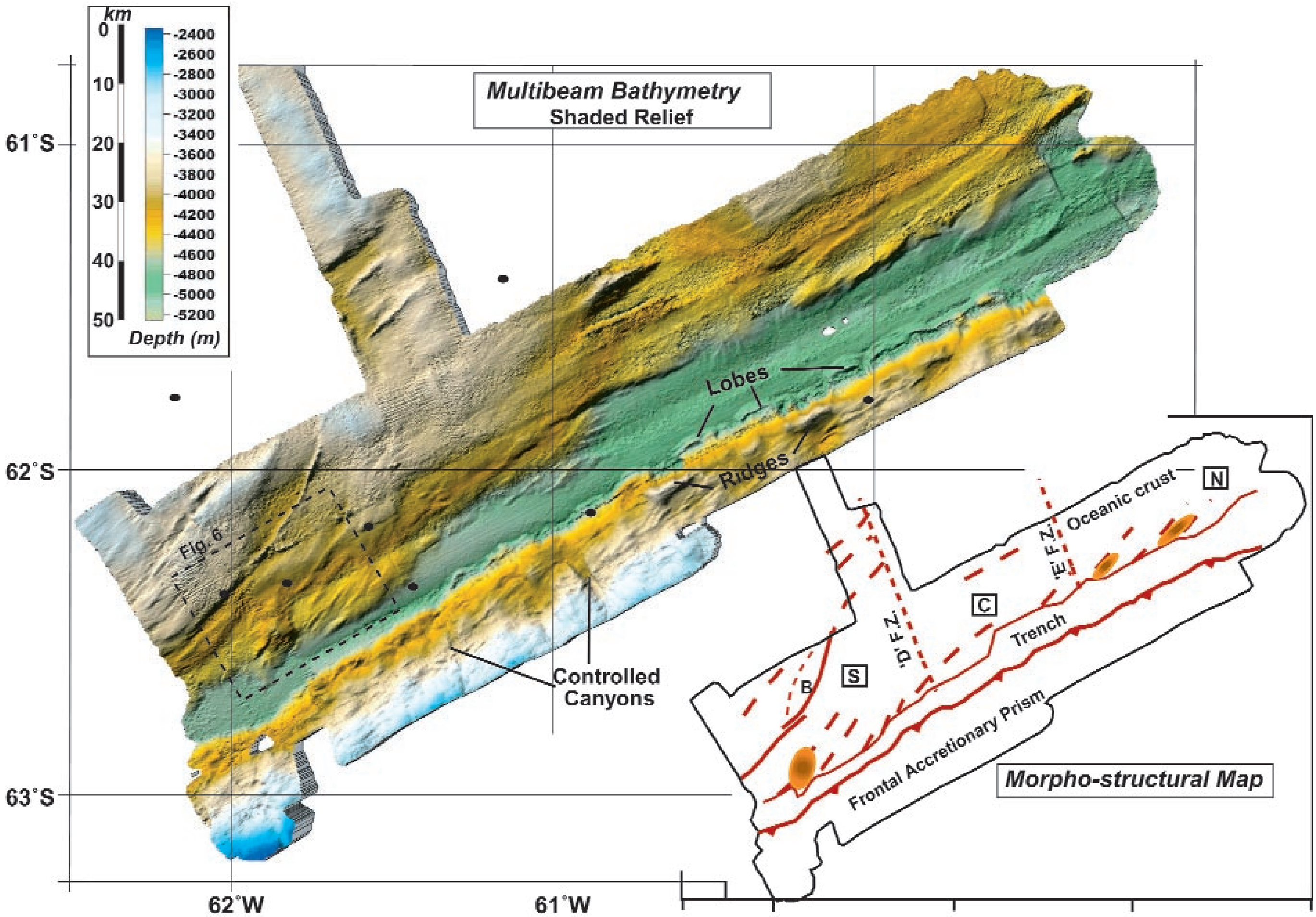

Fig. 5 - Shaded relief morpho-bathymetry image of the investigated area. The schematic morpho-structural interpretation is also shown. Solid orange ellipses indicate the volcanic edifices; B- half-graben basin. Black dots indicate earthquake events obtained from the web side http://epsc.wustl.edu/seismology/SEPA. Dasched box shows the location of figure 6.

affecting the last remnant PHO Plate and formed by normal faults, associated to horst and graben structures, that are obliquely oriented to the “E” and “D” FZs. The faults and the absence of sub-horizontal sediments on the edge of the Explora Volcano suggest that the activity of oblique faults and of the volcanic eruption is recent to present. Moreover, the activity of oblique faults is supported by recent earthquakes occurring near some of these morpho-structures (Fig. 5).

The “Explora” Volcano is coincident with a major extensional lineament within the Southern segment (Fig. 4a), and is cut by a normal fault (Fig. 6a), suggesting that recent tectonic activity followed its emplacement. The lobate morphology of the sea bottom close to the volcano is characterized by the absence of sub-horizontal sedimentary cover (Fig. 4a). This, combined with the magnetic anomaly signature, suggests that the activity is recent and favoured by the extensional tectonics. Unfortunately, it is not possible to date the age of the last eruption due to the lacking of any rock and sediment samples. The magnetic anomaly close to the volcano has a positive signature of about 200 nT (Fig. 6b), suggesting that the last eruption occurred during the normal Earth magnetic field. Other two seamounts, located within the Northern segment, are interpreted as small volcanoes and are characterized by an elongated shape oriented parallel to the oblique extensional lineaments (Fig. 5).

Oblique faults show significant offsets of the seafloor, mainly in the SW oceanic segment (Fig. 3), that become less pronounced close to the trench axis (Fig. 4) and toward the outer rise (Fig. 5). The fault offsets close to the trench could be masked by trench infill and distal bottom current sedimentary deposits, whereas the decreased offset toward the outer rise could be due to the less intense plate bending. On the base of the analysis of these geometric features it seems that the plate bending partially controls the activity of normal faults, as analysed along the Costa Rica margin (Ranero et al., 2003). The smooth morphology of the Central segment is affected by few lineaments oriented orthogonally to the “D” and “E” FZs (Figs. 2 and 5). These structural and morphological characters abruptly change in correspondence of the “D” and “E” FZs suggesting that they could act as mechanical discontinuities, causing different coupling that might increase the bending of the Central segment. Thus, we speculate that the crustal thickness, related to the different age of each single segment, cannot exhibit an appropriate expression, because of a significant change in the coupling at the ”D” and “E” FZs and at the PHO plate boundaries.

In the Southern and Northern oceanic segments the normal faults are oriented with a direction that forms a different angle with the continental margin strike (Fig. 2). This oblique normal faults system through the oceanic remnant does not appear to cut across the oceanic segment boundaries (Fig. 5), suggesting that the FZs act as a mechanical boundary to the propagation of the deformation (Figs. 2 and 5). The expression of these FZs may be masked by sedimentary deposits of trench and distal bottom current, similar to those south of Hero FZ (Camerlenghi et al., 1997; Rebesco et al., 2002). The oblique extensional pattern intersects the trench and shape the accretionary prism. The extensional character of the oblique trending faults, that form localized horst and graben structures (Kim et al., 1995), suggests that they are produced by the plate bending and by the presence of inherited oceanic spreading fabric or by pre-existing weak zones, as observed along other margins (Masson, 1991; Ranero et al., 2005). We hypothesize that the orientation of this normal faults system could be controlled by the different coupling along the transform faults; it is likely higher along Hero and Shackleton FZs and lower along “D” and “E” FZs, thus able to modify the stress field orientation.

Geological model

The seafloor depth and morphology suggest that the mechanical coupling along the two “E” and “D” FZs is not as strong as along the two main FZs (Hero and Shackleton). The combination of bending and retreat of the plate, with the strong coupling along the lateral boundaries of the PHO Plate, modifies the stress field from the Northern and Southern segments towards the Central one. The result is the development of horst and graben structures, associated to normal faults, showing variable orientation on the incoming segments, which tend to propagate backwards, in agreement with the roll-back of the subducting oceanic plate. The roll-back of the oceanic plate favours the opening of the Bransfield Strait back-arc basin, which might episodically induce compression at the South Shetland Trench.

The geological model that explains these features combines the effects of three main processes:

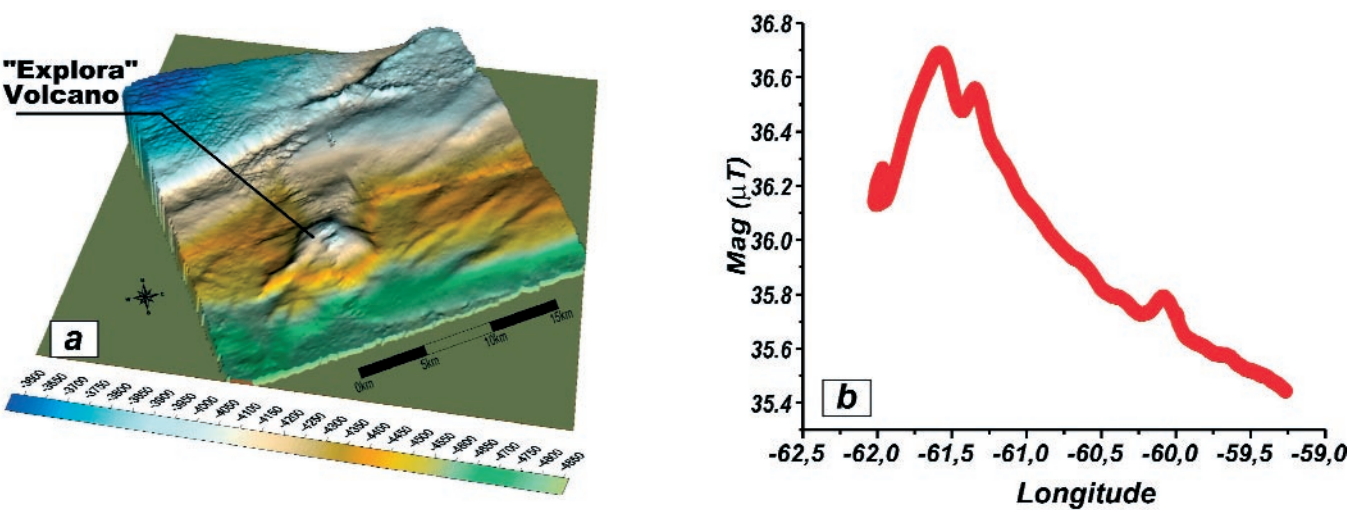

Fig. 6 - a: Detailed shaded relief morpho-bathymetry image in the area around the “Explora” Volcano. b: Magnetic profiles acquired in the area. The red profile is located along the Chirp line B1 and B2 (Fig. 2).

– the angle of incidence of the incoming oceanic subduction, composed by 3 oceanic segments that are characterized by different ages and thickness, with respect to the AP continental margin;
– the different coupling of FZs bounding the oceanic segments;
– the bending and roll-back of the oceanic plate that control the opening of Bransfield Strait and seaward migration of the Bransfield Microplate.

CONCLUSIONS

The analysis of new geophysical data acquired offshore the Antarctic Peninsula has highlighted shallow structures affecting the passive subducting Phoenix Plate and allowed the description of the morphology of the South Shetland Trench. In particular, the new multibeam image shows in detail the character and extension of the main investigated domains, that are the incoming oceanic crust, the trench, and the frontal AP accretionary prism.

The incoming oceanic plate is affected by a normal fault system characterized by an orientation ranging from parallel to oblique with respect to the trench axis. Basins, horst and graben structures are located in correspondence of these oblique normal faults that are controlled by: (1) the bending of the oceanic plate; (2) the presence of inherited oceanic spreading fabric or pre-existing weak zones; (3) the presence of mechanical discontinuities as “D” and “E” Fracture Zones, characterized by a different coupling, that modifies the stress field orientation. We detect a new seamount called “Explora” Volcano not covered by oceanic sediments and deformed by a normal fault, and thus dating the normal faults activity as recent.

The trench narrows southwards, deepens north-ward, and shows a sharp bend trend of the outboard side. The morphology is controlled by several elements such as: the normal faults system; the presence of “D” and “E” Fracture Zones; the different plate bending of the three oceanic segments controlled by the main Hero and Shackleton Fracture Zones; and the interaction of a morphological anomaly, i.e. the “Explora” Volcano.

ACKNOWLEDGEMENTS

We are very grateful to S. Libralato, D. Brunelli and M. Ligi for constructive criticisms. A thankful review F. Ferraccioli, D. Fontana and C.R. Ranero helped to improve the manuscript. This study would not have been possible without the support of the crew and technicians of the R/V OGS-Explora during the field acquisition. This work was supported by Italian *Programma Nazionale di Ricerche in Antartide (PNRA)*, SLAPPSS program.

REFERENCES

Aldaya F. and Maldonado A., 1996. Tectonics of the triple junction at the southern end of the Shackleton Fracture Zone (Antarctic Peninsula). Geo-Marine Lett., 16: 279-286.

Ballance P.F., Scholl D.W., Vallier L.T., Stevenson A.J., Ryan H. and Herzer R.H., 1989. Subduction of a late Cretaceous seamount of the Louisville ridge at the Tonga trench: a model of normal and accelerated tectonic erosion. Tectonics, 8 (5): 953-962.

Barker P.F. and Dalziel I.W.D., 1983. Progress in geodynamics in the Scotia Arc region. In: R. Cabre (Ed.), Geodynamics of the Eastern Pacific region, Caribbean and Scotia Arcs. AGU, Washington, DC, Geodyn. Ser., p. 137-170,

Barker P.F., 1982. The Cenozoic subduction history of the Pacific margin of the Antarctic Peninsula: Ridge crest-trench interactions. J. Geol. Soc. London, 139: 787-801.

Camerlenghi A., Crise A., Accerboni E., Laterza R., Pudsey C.J. and Rebesco M., 1997. Ten-mouth observation of the bottom current regime across a sediment drift of the Pacific margin of the Antarctic Peninsula. Antarctic Sci., 9 424-431.

Carbotte S.M. and Macdonald K.C., 1994. Comparison of seafloor tectonic fabric at the intermediate, fast, and super fast spreading ridges: Influence of spreading rate, plate motions, and ridge segmentation on fault patterns. JGR, 99 (B7): 13,609-13,631.

Cohen J.K and Stockwell Jr.J.W., 2003. CWP/SU: Seismic Unix Release 37: a free package for seismic research and processing. Center for Wave Phenomena, Colorado School of Mines.

Dietrich R., Dach R., Engelhardt G., Ihde J., Korth W., Kutterer H.-J., Lindner K., Mayer M., Menge F., Miller H., Müller C., Niemeier W., Perlt J, Pohl M., Salbach H., Schenke H.-W., Schöne T., Seeber G., Veit A. and Völksen C., 2001. ITRF coordinates and plate velocities from repeated GPS campaigns in Antarctica-An analysis based on different individual solutions. J. Geodesy, 74: 756-766.

Dominguez S., Malavieille J. and Lallemand S.E., 2000. Deformation of accretionary wedges in response to seamount soubduction: Insight from sandbox experiments. Tectonics, 19 (1): 182-196.

Fisher D.M., Gardner T.W., Marshall J.S., Sak P.B. and Protti M., 1998. Effect of subducting sea-floor roughness on fore-arc kinematics, Pacific coast, Costa Rica. Geology, 26 (5): 467-570.

GRAPE Team, 1990. Preliminary results of seismic reflection investigations and associated geophysical studies in the area of the Antarctic Peninsula. Antarctic Sci., 2: 223-234.

Gulick S.P.S., Bangs N.L.B., Shipley T.H., Nakamura Y., Moore G. and Kuramoto S., 2004. Three-dimensional architecture of the Nankai accretionary prism’s imbricate thrust zone off Cape Muroto, Japan: Prism reconstruction via en echelon thrust propagation. JGR, 99 (B02105): doi: 10.1029/2003JB002654.

Hawkes D.D., 1981. Tectonic segmentation of the northern Antarctic Peninsula. Geology, 9: 220-224.

Hilde T.W.C., 1983**.** Sediment subduction vs. accretion around the Pacific. Tectonophysics, 99: 381-397.

Huyghe P., Foata M., Deville E., Mascle G. and Caramba Working Group, 2004. Channel profiles through the active thrust front of the southern Barbados prism. Geology, 32 (5): 429-432.

Kim Y., Kim H.-S., Larter R.D., Camerlenghi A., Gambôa L.A.P. and Rudowski S., 1995. Tectonic deformation in the upper crust and sediments at the South Shetland Trench. In: A.K. Cooper, P.T. Barker and G. Brancolini (Eds), Geology and seismic stratigraphy of the Atlantic Margin. AGU, Washington, DC, Antarct. Res. Ser., 68: 157-166.

Kobayashi K., Nakanishi M., Tamaki K. and Ogawa Y., 1998. Outer slope faulting associate with the western Kuril and Japan trenches. Geophys. J. Int., 134: 356-372.

Kuvaas B., Kristoffersen Y., Guseva J., Leitchenkov G., Gandjudhin V., Løvås O., Sand M. and Brekke H., 2005. Interplay of turbidite and contourite deposition along the Cosmonaut Sea/Enderby Land margin, East Antarctic. Marine Geol., 217: 143-159.

Lallemand S.E., Schnürle P. and Malavieille J. 1994. Coulomb theory applied to accretionary and non-accretionary wedges: Possible causes for tectonic erosion and/or frontal accretion. J. Geophys. Res., 99 (B6): 12033-12055.

Larter R.D. and Barker P.F., 1991. Effects of ridge crest-trench inter-action on Antarctic-Phoenix spreading: forces on a young subducting plate. J. Geophys. Res., 96: 19,583-19,607.

Larter R.D., 2001. Cenozoic tectonic history, seismicity and palaeoseismicity of the Antarctic Peninsula Pacific margin. Terra Antartica, 8 (2): 79-86.

Lawver L.A., Keller R.A., Fisk M.R. and Strelin J.A., 1995. Bransfield Strait, Antarctic Peninsula: Active extension behind a dead arc. In: B.Taylor (Ed.), Back arc basin: Tectonics and magmatism volume. Amsterdam Plenum Press, p. 315-342.
Lodolo E., Camerlenghi A., Madrussani G., Tinivella U. and Rossi G., 2002. Assessment of gas hydrate and free gas distribution on the South Shetland margin (Antarctica) based on multichannel seismic reflection data. Geophys. J. Int., 148: 103-119.
Loreto M.F., 2005. Analisi dei processi di subduzione della Placca Antartica al largo della Terra del Fuoco (Cile Meridionale). PhD thesis, Univ. of Parma, Italy, 122 pp.
Masson D.G., 1991. Fault patterns at outer trench walls. Mar. Geophys. Res., 13: 209-225.
Morley C.K., 2001. Combined escape tectonics and subduction rollback-arc extension; a model for the evolution of Tertiary rift basins in Thailand Malaysia and Laos. J. Geol. Soc. London, 158: 461-474.
Nemcok M., Pospissil L., Lexa J. and Donelick R.A., 1998. Tertiary subduction and slab break-off model of the Carpathian-Pannonian region. Tectonophysics, 295: 307-340.
Pankhurst R.J., 1990. The Paleozoic and Andean magmatic arcs of West Antarctica and southern South America. In: S.M. Kay and C.W Rapela (Eds.), Plutonism form Antarctica to Alaska. Geol. Soc. Am. Spec. Pap., 241: 1-7.
Pelayo A.M. and Wiens D.A., 1989. Seismotectonics and relative plate motions in the Scotia Sea region. J. Geoph. Res., 94 (B6): 7293-7320.
Pudsey C.J. and Camerlenghi A., 1998. Glacial-Interglacial deposition on a sediment drift on the Pacific margin of the Antarctic Peninsula. Antarctic Sci., 10: 1-23.
Ranero C.R. and von Huene R., 2000. Subduction erosion along the Middle America convergent margin. Nature, 404: 748-752.
Ranero C.R., Morgan J.P., McIntosh K. and Reichert C., 2003. Bending-related faulting and mantle serpentinization at the Middle America trench. Nature, 425: 367-373.
Ranero C.R., Villaseñor A, Morgan J.P and Weinrebe W., 2005. Relationship between bend-faulting at trenchs and intermediate-depth seismicity. Geoch. Geoph. Geosys., 6 (12), Q12002, doi: 10.1029/2005GC000997.
Rebesco M., Pudsey C.J., Canals M., Camerlenghi A., Barker P.F., Estrada F. and Giorgetti A., 2002. Sediments drifts and deep-sea channel systems, Antarctic Peninsula Pacific margin. In: D.A.V Stow., C.J. Pudsey, J.A. Howe, J.-C. Faugères and A.R. Viana (Eds.), Deep-water contourite systems: Modern drifts and ancient series, seismic and sedimentary characteristics. Geol. Soc. London Mem., 22: 353-371.
Robertson Maurice S.D., Wiens D.A., Shore P.J., Vera E. and Dorman LeR. M., 2003. Seismicity and tectonics of the South Shetland Islands and Bransfield Strait from a Regional broadband seismograph deployment. J. Geophy. Res., 108 (B10): 2461, doi: 10.1029/2003JB002416.
Royden L.H., 1988. Late Cenozoic tectonics of the Pannonian basin system. In: L. Royden and F: Horváth (Eds). The Pannonian Basin: A Study in Basin Evolution, Mem. AAPG, 45: 27-48.
Royden L.H., 1993. The tectonic expression slab pull at continental convergent boundaries. Tectonics, 12 (2): 303-325.
Sandwell D.T. and Smith W.H.F., 1997. Marine gravity anomaly from Geosat and ERS-1 satellite altimetry. J.G.R. (B), 102 (5): 10,039-10,054.
Scholl D.W., Christense M.N., von Huene R. and Marlow M.S., 1970. Peru-Chile trench sediments and sea-floor spreading. Geol. Soc. Am. Bull., 81: 1339-1360.
Schweller W.J. and Kulm L.K., 1978. Extensional rupture of oceanic crust in the Chile Trench. Marine Geol., 28: 271-291.
Smalley R., Jr., Kendrick E., Bevis M.G., Dalziel I.W.D., Taylor F., Lauría E., Barriga R., Casassa G., Olivero E., Piana E., 2003. Geodetic determination of relative plate motion and crustal deformation across the Scotia-South America plate boundary in eastern Tierra del Fuego. Geochem. Geophys. Geosyst., 4(9): 1070, DOI 10.1029/2002GC000446.
Thomas C., Livermore R. and Pollitz F., 2003. Motion of the Scotia Sea Plates. Geophys. J. Int., 155: 789-804.
von Huene R. and Ranero C.R., 2003. Subduction erosion and basal friction along the sediment starved convergent margin off Antofagasta, Chile. J.G.R., 108 (B2): 2079, doi: 10.1029/2001JB001569.
von Huene R., 1986. To accrete or not accrete, that is the question. Geol. Runds., 75 (1): 1-15.

Received, February 24, 2006
Accepted, July 18, 2006